JOURNAL OF VIROLOGY, Oct. 1992, p. 5898–5905
0022-538X/92/105898-08$02.00/0

Vol. 66, No. 10

The Fitness of Defective Interfering Murine Coronavirus DI-a and Its Derivatives Is Decreased by Nonsense and Frameshift Mutations

RAOUL J. DE GROOT, ROBERT G. VAN DER MOST, AND WILLY J. M. SPAAN*

Department of Virology, Institute of Medical Microbiology, Faculty of Medicine, Leiden University, P.O. Box 320, 2300 AH Leiden, The Netherlands

Received 18 May 1992/Accepted 29 June 1992

The genome of the defective interfering (DI) mouse hepatitis virus DI-a carries a large open reading frame (ORF) consisting of ORF1a, ORF1b, and nucleocapsid sequences. To test whether this fusion ORF is important for DI virus replication, we constructed derivatives of the DI-a genome in which the reading frame was truncated by a nonsense codon or a frameshift mutation. In vitro-transcribed DI RNAs were transfected into mouse hepatitis virus-infected cells followed by undiluted passage of the resulting virus-DI virus stocks. The following observations were made. (i) Truncation of the fusion ORF was not lethal but led to reduced accumulation of DI RNA. (ii) When pairs of nearly identical in-frame and out-of-frame DI RNAs were directly compared by cotransfection, DI viruses containing in-frame genomic RNAs prevailed within three successive passages even when the out-of-frame RNAs were transfected in 10-fold molar excess. (iii) When DI viruses containing out-of-frame genomic RNAs were passaged, mutants emerged and were selected for that had restored the reading frame. We conclude that translation of the fusion ORF is indeed required for efficient propagation of DI-a and its derivatives.

High-multiplicity propagation of viruses frequently results in the formation of defective interfering viruses (DIs). DIs contain truncated genomes that have lost most of their protein-encoding potential but have preserved the essential replication signals (7, 10–12). For propagation, DIs thus depend on the replication machinery and the structural proteins provided by the standard virus. In fact, by competing with the standard virus for replication requirements, DIs interfere with virus growth and cause reduced virus yields.

DIs have also been described for coronaviruses, a group of enveloped RNA viruses (9, 19, 25, 38). Mouse hepatitis virus (MHV), the best-studied member of this family, contains a single-stranded, plus-sense RNA genome of 32 kb (16, 31). The MHV DI genomes characterized so far are of the internal deletion type (10), i.e., the 5′ and 3′ termini are retained, but multiple internal segments of the standard virus genome are deleted (19, 24, 26, 38).

For three different MHV DI genomes, full-length DNA copies have been cloned downstream of the phage T7 promoter. RNAs transcribed from these constructs in vitro were found to be replicated efficiently when introduced into MHV-infected cells (3, 22, 38). These synthetic DI RNAs have proved to be valuable tools for studies on various aspects of coronavirus replication, such as leader switching (22) and transcription initiation (20). Their use also allowed the identification of an encapsidation signal (3, 38). Moreover, synthetic DI RNAs provide a means to site-specifically introduce mutations in the MHV genome via homologous RNA recombination (39).

An intriguing aspect of DIs is their extremely rapid evolution (7, 32). During propagation, the MHV DI genomes appear to undergo progressive modifications, notably insertions and deletions, and new DIs emerge only to be succeeded by other, more efficiently replicating species (19, 38). The factors that determine the fitness of MHV DIs are poorly understood, although a small size of the DI genome and the presence of an encapsidation signal seem to provide distinct selective advantages (19, 24, 26, 38). Interestingly, the genomic RNAs of the natural MHV DIs DIssE (24) and DI-a (38) consist of noncontiguous fragments of the MHV genome that have been fused in-frame. Consequently, DI-a and DIssE carry a single open reading frame (ORF) spanning almost their entire genome. This observation prompted us to consider a possible role of the fusion ORF in DI replication. Here, we show, by introduction of nonsense and frameshift mutations, that the fusion ORF is indeed required for efficient propagation of DI-a and its derivatives.

MATERIALS AND METHODS

Cells and tissue culture. Mouse L cells were grown in Dulbecco's modified Eagle's medium supplemented with 10% fetal calf serum. A concentrated virus stock of MHV strain A59 prepared by polyethylene glycol 6000 precipitation (36) was used. Transfection of in vitro-transcribed DI RNA was performed as described by van der Most et al. (38).

Recombinant DNA techniques. Standard procedures were used for recombinant DNA techniques (2, 33). DNA sequence analysis was performed with T7 DNA polymerase (Pharmacia) according to the instructions of the manufacturer.

Isolation and analysis of viral RNAs. Intracellular and viral genomic RNA was isolated as described by Spaan et al. (36). RNA was separated in 2.2 M formaldehyde–1% agarose gels (34). The gels were dried and hybridized with 5′-end-labeled oligonucleotide probe 12 (Table 1) as described by Meinkoth and Wahl (28).

Construction of plasmids. (i) pMIDI-C and pMIDI-U. Silent marker mutations were introduced in pMIDI (38) at positions 1778 (G→A, mutation A), 2297 (T→C, mutation B), and 3686

* Corresponding author.

TABLE 1. Oligonucleotide sequences used

Oligonucleotide	Sequence	Polarity	Binding site in MIDI-U/C	Binding site in ΔH-*in*
1	5′ ATTATGTCCAGCACAAGTGTG 3′	+	1744–1764	1744–1764
2	5′ ACGTGTACTCCAGCACACGTC 3′	−	3894–3914	
3	5′ GTGATTCTTCCAATTGGCCATG 3′	−	5473–5494	3409–3430
4	5′ TGGCAATCTCGAGCAAAGAGCTATC 3′	+	1763–1787	1763–1787
5	5′ AACGAAATTCTTGACAAGCTC 3′	−	2280–2300	
6	5′ GCTCTTAACTAGTTTATCCACAAAG 3′	−	3677–3701	
7	5′ ACCGACATAGAGTCGATC 3′	−	2330–2347	
8	5′ TTGCGCATACTGGTAGTC 3′	+	3190–3207	
9	5′ TATTTGATTAAGAGTGGTCGA 3′	+	1965–1985	1965–1985
10	5′ TTTTATGGATTTAGATGATG 3′	+	4382–4401	2318–2337
11	5′ CCAATTCTAATTTAGATCCA 3′	−	4808–4827	2744–2763
12	5′ TTCCTGAGCCTGTCTACG 3′	−	5019–5036	2955–2972

(C→T, mutation D) by polymerase chain reaction (PCR) mutagenesis (33), using oligonucleotide primers 4, 5, and 6 (Table 1) and pMIDI DNA as the template. The *Xho*I-*Hin*cII (1770 to 2298) and *Xho*II-*Spe*I (3237 to 3689) fragments derived from the resulting PCR products were used to replace the corresponding fragments in pMIDI, yielding pMIDI-U. pMIDI-U contains a serendipitous C→T substitution at position 3357 which gives rise to a UAA termination codon. pMIDI-C also carries the genetic markers A, B, and D (39), but the UAA stop codon is replaced by the wild-type sequence CAA. Furthermore, pMIDI-C carries an additional silent mutation (T→C) at position 3572 (mutation C). All cloned PCR DNA fragments in pMIDI-U and pMIDI-C were sequenced as were the junctions created by ligation. No other mutations were found.

(ii) pΔH-*in* and pΔH-*out*. Plasmid pMIDI was digested with *Hin*dIII (positions 1985 and 4040), treated with 5 U of S1 nuclease for 15 min at 37°C, and religated. The resulting pMIDI derivatives were sequenced by using oligonucleotide primer 4 (Table 1). Two clones were selected in which S1 nuclease had not only deleted the 5′ protruding ends of the *Hin*dIII sites, but also 5 (pΔH-*in*) or 6 (pΔH-*out*) nucleotides of the flanking sequences, thus yielding two pMIDI derivatives that differ only by a single nucleotide.

(iii) pΔH-*Mlu* and pΔH-*Spe*. pΔH-*in* DNA was digested with *Mlu*I or *Spe*I, and the 3′ recessed ends were filled in with Klenow DNA polymerase and then religated. This yielded pΔH-*Mlu* and pΔH-*Spe*, respectively. To confirm the mutations, pΔH-*Mlu* was sequenced with oligonucleotide primer 10 (Table 1), and for sequene analysis of pΔH-*Spe*, primer 11 (Table 1) was used.

cDNA synthesis and PCR amplification (RT-PCR). To analyze MIDI-U RNA after replication, we separated intracellular RNA from cells infected with passage 2 virus-DI mixture (see Fig. 2a) on a nondenaturing, low-melting-point, 1% agarose gel. The DI RNA was excised and isolated as described elsewhere (33). First-strand cDNA synthesis was performed with RNase H-free Moloney murine leukemia virus reverse transcriptase (BRL, Life Technologies); this was followed by PCR amplification with *Taq* polymerase (Promega) according to the instructions of the manufacturer. Oligonucleotides 1 and 2 were used. The generated PCR DNA was cut with *Hin*dIII (nucleotides 1985 and 3782), the 1.8-kb fragment was cloned into *Hin*dIII-digested pUC20, and this was followed by $CaCl_2$ transformation of *Escherichia coli* HB101. To ensure that the resulting bacterial colonies were independent, the cells were recovered for only 30 min at 37°C after heat shocking.

Analysis of in-frame escape mutant DI RNAs. RT-PCR analysis of in-frame escape mutants derived from ΔH-*out* and *swop*1 to -3 was performed with unfractionated p3 RNA and oligonucleotide primers 1 and 3. DI-specific fragments were generated with the expected length of 1.7 kb. These fragments were purified from low-melting-point agarose gels (33) and digested with *Taq*I, after which the 3′ recessed ends were filled in with Klenow DNA polymerase, [^{32}P]dCTP (3,000 Ci/mmol; Amersham), and unlabeled dATP, dGTP, and dTTP. The restriction fragments were analyzed in nondenaturing TBE (89 mM Tris-borate, 2 mM EDTA [pH 8.0])–5% polyacrylamide gels (33). For sequence analysis, the PCR fragments were digested wtih *Bss*HII and *Sac*I, and the resulting 1,477-bp fragment was cloned into *Mlu*I-*Sac*I-digested pUC21. For each DI mutant, 12 independent recombinant plasmids were isolated and characterized by restriction analysis and then sequence analysis with the universal sequencing primer and oligonucleotide 9.

In vitro translation and immunoprecipitation. In vitro translation was performed in a 10-μl reaction mixture containing nuclease-treated, methionine-depleted rabbit reticulocyte lysate (Promega), supplemented with 10 μCi of [^{35}S]methionine (>1,000 Ci/mmol; Amersham), 20 μM unlabeled amino acid mixture lacking methionine (Promega), and 10 to 50 ng of in vitro-transcribed RNA or cytoplasmic RNA from the equivalent of 10^5 infected cells. The labeled proteins were immunoprecipitated as described by Baker et al. (4), using antisera raised against synthetic peptides derived from the N terminus of MHV ORF1a (4) or the C terminus of the MHV N protein (kindly provided by K. V. Holmes). The immunoprecipitated products were analyzed by electrophoresis in sodium dodecyl sulfate (SDS)–7.5% polyacrylamide gels.

RESULTS

Termination codon in MIDI genome is removed via homologous recombination. We previously reported the construction of pMIDI, a DNA copy of the DI-a genome from which RNA can be transcribed in vitro (38). As shown schematically in Fig. 1, the DI-a genomic RNA consists of the following noncontiguous parts of the MHV-A59 genome: the 5′-most 3,889 nucleotides containing the 5′ noncoding region and part of ORF1a, a 799-nucleotide middle segment derived from ORF1b, and 806 nucleotides encompassing the 3′ end of the nucleocapsid (N) gene and the 3′ noncoding region. In the present study, two pMIDI derivatives were used, pMIDI-C and pMIDI-U. As shown in Fig. 1, MIDI-C RNA

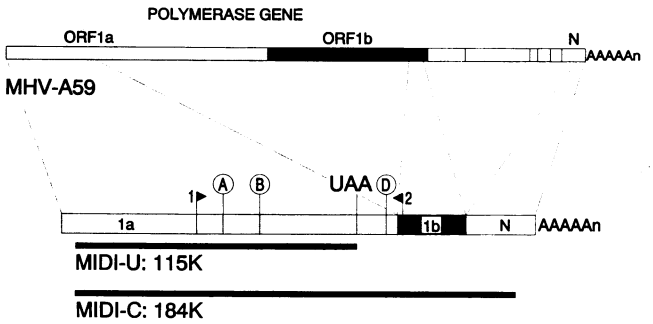

FIG. 1. Schematic representation of the structure of MIDI-U, MIDI-C, and the MHV-A59 genome. The parts of the DI RNAs derived from the 5′ end (ORF1a), ORF1b, and the 3′ end (N) of the MHV-A59 genome are depicted as boxes with different shading. The locations of the silent marker mutations A, B, and D are shown. Also indicated are the UAA termination codon in MIDI-U and the positions of oligonucleotides 1 and 2 used for RT-PCR. The ORFs of MIDI-U and MIDI-C, coding for the 115K and 184K polypeptides, respectively, are depicted as black bars. MIDI-C contains an additional silent mutation (marker C) at position 3572 (not indicated, [39]).

carries an ORF for a 184,000-molecular-weight hybrid polypeptide (184K polypeptide), which spans almost the entire DI RNA and leaves only the 5′ and 3′ noncoding regions untranslated. This type of fusion ORF will be referred to below as full length. In MIDI-U, the ORF is truncated by a UAA termination codon in the ORF1a sequence and codes for a polypeptide of only 115,000 molecular weight (115K polypeptide). MIDI-C and MIDI-U both contain silent point mutations in the ORF1a sequence that serve as genetic markers (Fig. 1) (39).

To evaluate the role of the ORF in DI propagation, we used RNAs derived from pMIDI-U and pMIDI-C for transfection of MHV-infected cells. As a control, MHV-infected cells were mock transfected with phosphate-buffered saline. Progeny virus was harvested and passaged twice in fresh L cells. Figure 2a presents an outline of the experiments and explains the nomenclature of virus stocks and RNA preparations. Intracellular RNAs from the different passages were separated in denaturing formaldehyde-agarose gels and hybridized to oligonucleotide 12 (Table 1). This probe detects all MHV mRNAs in addition to the DI RNAs. As shown in Fig. 2b, both MIDI-U and MIDI-C were replicated, but MIDI-C accumulated to higher levels and displayed a much stronger interference with viral replication. During passage, endogenous DI RNAs emerged, the most predominant of which, DI-*en* RNA, is also indicated in Fig. 2b. Interestingly, DI-*en* was rapidly outcompeted by MIDI-C, but accumulated to large amounts after initial transfection of MIDI-U RNA.

To study the fate of the termination codon in MIDI-U RNA, we translated p1 and p2 RNAs in rabbit reticulocyte lysates. The DI-encoded polypeptides were immunoprecipitated with αP28 serum. This serum specifically binds to P28, a protein which is derived from the N terminus of the viral ORF1a product by proteolytic cleavage in *cis* (4–6). The active site of the *cis*-acting proteinase is not encoded by the MIDI-U and MIDI-C RNAs, and therefore, cleavage of the DI-encoded polypeptides does not occur (4, 24, 26). As shown in Fig. 2c, translation of p1 MIDI-U RNA yielded predominantly the expected 115K polypeptide, but in addition, a product was found that comigrated with the 184K

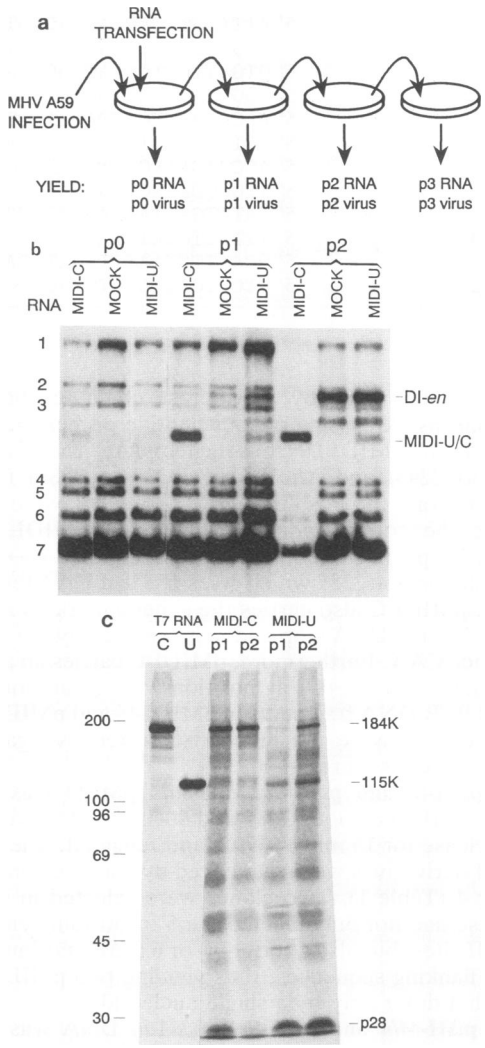

FIG. 2. Transfection-propagation of MIDI-U and MIDI-C DI RNAs in MHV-infected L cells. (a) Schematic outline of the experiment showing the transfection of MHV-infected cells with synthetic DI RNAs and the undiluted passage of the resulting virus-DI stocks. The nomenclature used for virus stocks and intracellular RNA preparations is explained. (b) Analysis of intracellular RNAs. MHV-A59-infected L cells were transfected with in vitro-transcribed MIDI-C or MIDI-U RNA or were mock transfected with phosphate-buffered saline. The resulting virus stocks were harvested and passaged twice on fresh L cells. p0, p1, and p2 RNAs were isolated and separated in formaldehyde-agarose gels and hybridized to 5′-end-labeled oligonucleotide 12. The MIDI-U, MIDI-C, and DI-*en* RNAs are indicated as well as the MHV mRNAs. (c) Translation in vitro of p1 and p2 RNAs. The intracellular p1 and p2 RNA preparations shown in panel B were translated in vitro in rabbit reticulocyte lysate in the presence of [^{35}S]methionine. Labeled proteins were immunoprecipitated with an antiserum (αP28) specific for the N terminus of the ORF1a product and separated in SDS-7.5% polyacrylamide gels followed by fluorography. The 184K and 115K proteins translated from synthetic MIDI-C and MIDI-U RNA, respectively, were used as markers. Numbers on the left show molecular weights in thousands.

TABLE 2. Elimination of marker mutations[a]

Marker mutation	Position	No. of clones restored by wild-type sequence (n = 34)	%
Marker B	2297	28	81
UAA codon	3357	26	75
Marker D	3686	10	29

[a] PCR DNA derived from p2 MIDI-U RNA was prepared as described in the text, digested with *Hin*dIII, and cloned into pUC20. Thirty-four independent PCR clones were sequenced with oligonucleotide 7 (marker B), the universal- and the reverse-sequence primers (marker D), and oligonucleotide 8 (UAA codon). The number of clones in which the mutation is restored by the wild-type sequence is presented. Marker A was not analyzed.

polypeptide encoded by MIDI-C. In fact, after translation of p2 MIDI-U RNA, the 115K polypeptide and the larger protein were present in about equal amounts. Neither of these products was observed after translation of p2 mock RNA (data not shown), indicating that these polypeptides are specific for the MIDI derivatives. No DI-*en*-specific translation product was detected. Possibly, this product is processed, which would also explain the large amount of P28 observed after translation of p2 MIDI-U RNA (Fig. 2c).

Apparently, during passage of MIDI-U, mutant DI viruses accumulated that had eliminated the termination codon. The fact that the larger polypeptide, but not the 115K product, could be precipitated by using an antiserum against the nucleocapsid protein strongly supported this idea (not shown). The most likely possibility was that MIDI-U sequences had been replaced by sequences derived from the standard virus genome via homologous RNA recombination, thus restoring the full-length ORF (15, 21, 39). To study this, p2 MIDI-U RNA was gel purified and subjected to cDNA synthesis and then PCR (RT-PCR) with oligonucleotides 1 and 2. Sequence analysis of cloned RT-PCR DNA suggested that in the majority of MIDI-U RNAs, the termination codon had been replaced by the wild-type sequence CAA. The genetic markers were replaced by wild-type nucleotides as well (Table 2), suggesting that indeed RNA recombination with the viral genome had occurred. The combined data provided a first indication that truncation of the ORF impaired DI virus propagation.

Effects of premature termination of translation on DI RNA replication. To study the role of a full-length ORF more precisely, we constructed two pMIDI derivatives, pΔH-*in* and pΔH-*out*, by cutting pMIDI with *Hin*dIII and then performing S1 nuclease digestion and religation. Thus, a 2.1-kb deletion was made and new ORF1a/1b junctions were created. The resulting DI RNAs are identical except for a 1-nucleotide difference at the ORF1a/1b junction (Fig. 3a). In ΔH-*in*, the ORF1a/1b sequences are fused in frame, generating a full-length reading frame for a 110-kDa polypeptide (110K polypeptide). ΔH-*out*, however, contains a truncated ORF for a polypeptide of 66 kDa (66K polypeptide) that terminates 53 nucleotides downstream of the ORF1a/1b junction. Note that for ΔH-*out*, the full-length ORF can only be restored by frameshift mutations and not via homologous recombination with the viral genomic RNA.

To test whether the truncated ORF decreases the fitness of ΔH-*out*, we designed a competition assay in which mixtures of in vitro-transcribed ΔH-*out* and ΔH-*in* RNAs were used for a transfection-propagation experiment (for an outline, see Fig. 2a). The ΔH-*out* and ΔH-*in* DNA templates were mixed 1:1, 10:1, and 1:10 before transcription in vitro by T7 RNA polymerase. We explicitly chose to mix the DNA templates rather than the T7 transcripts to ensure that the competing DI RNAs were of equal quality. In vitro translation of the T7 transcripts confirmed that the RNAs were synthesized in the desired ratios (Fig. 3b). These RNA preparations were then used to transfect MHV-infected cells, and the resulting virus-DI stocks were passaged twice in fresh L cells. To determine which of the DIs was propagated best, p3 RNA (Fig. 2a) was isolated and translated in vitro. The DI-encoded polypeptides were immunoprecipitated with αP28 serum. The results show that ΔH-*in* was propagated much better than ΔH-*out*; even when ΔH-*out*

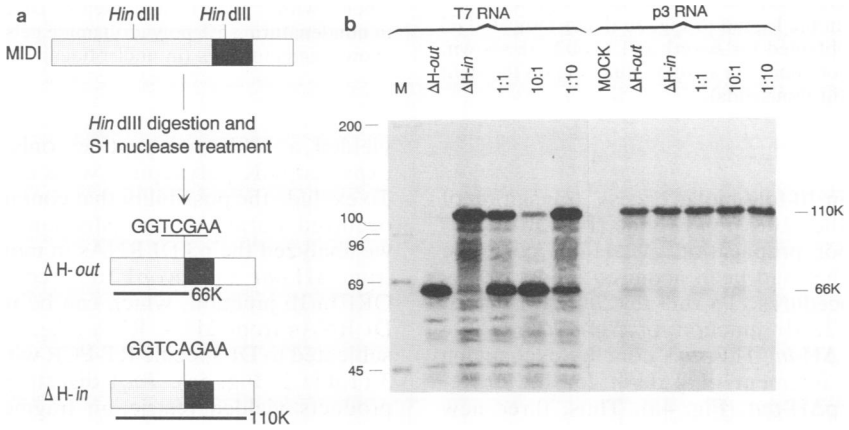

FIG. 3. Transfection-propagation of ΔH-*in* and ΔH-*out*. (a) Construction of ΔH-*in* and ΔH-*out*. pMIDI DNA was digested with *Hin*dIII, treated with S1 nuclease, and religated, giving rise to ΔH-*in* and ΔH-*out*. Sequences derived from different parts of the MHV genome are indicated by shaded boxes as in Fig. 1. The ORFs encoding the 66K and 110K polypeptides are depicted as black bars. Also indicated is the nucleotide sequence at the new ORF1a/1b junction; the *Taq*I site in ΔH-*out* DNA is underlined. (b) In vitro translation of synthetic and p3 RNAs in rabbit reticulocyte lysates. pΔH-*out* and pΔH-*in* DNA, either separately or mixed in the indicated ratios (ΔH-*out*: ΔH-*in*), was transcribed by using T7 RNA polymerase. The resulting RNAs were translated in rabbit reticulocyte lysate as described in the legend to Fig. 2c. The labeled proteins were directly analyzed by SDS-polyacrylamide gel electrophoresis (PAGE) (lanes T7 RNA). The synthetic RNA preparations were then used for a (co)transfection-propagation experiment as in Fig. 2a. The p3 RNAs were extracted and translated in vitro. Labeled proteins were immunoprecipitated with αP28 antiserum (lanes p3 RNA). Lane M, molecular weight markers (×10^3).

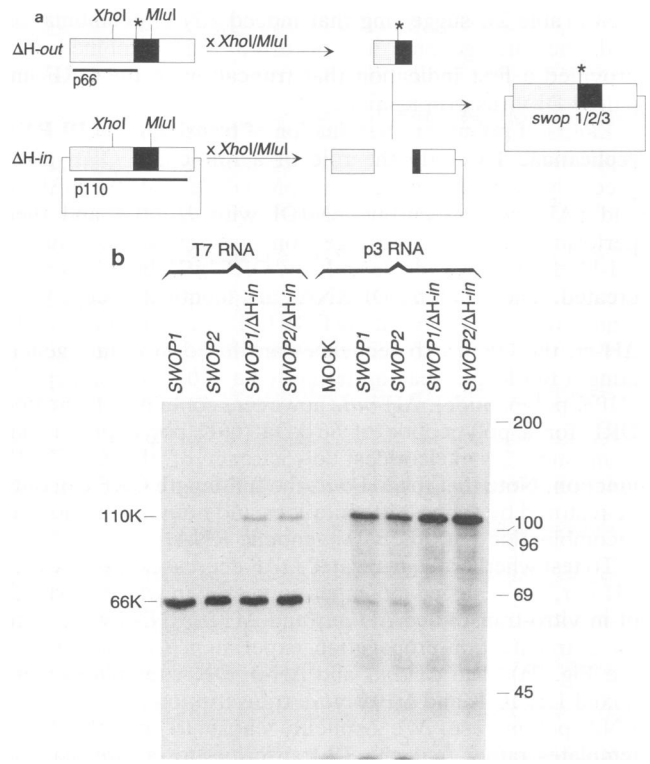

FIG. 4. (a) Construction of *swop*1 to -3. The *Xho*I-*Mlu*I fragment of ΔH-*out* spanning the ORF1a/1b junction was introduced into the genetic background of ΔH-*in*. ORFs are depicted as black bars; the termination codon of the ORF in ΔH-*out* is indicated by an asterisk. Sequence analysis confirmed that the *Xho*I-*Mlu*I fragments of ΔH-*in* and ΔH-*out* are identical except for the 1a/1b junction. (b) In vitro translation of synthetic and p3 *swop* DI RNAs. p*swop* DNA was transcribed, either separately or mixed in 10-fold excess with pΔH-*in* DNA, with T7 RNA polymerase. The synthetic RNAs were translated in rabbit reticulocyte lysate, and the translation products were analyzed by SDS-PAGE (lanes indicated T7 RNA). Subsequently, these RNAs were used for a (co)transfection-propagation experiment as explained in the legend to Fig. 2a. In vitro translation products of p3 RNAs were analyzed by immunoprecipitation and SDS-PAGE as described in the legend to Fig. 3b (lanes indicated p3 RNA). Only the results obtained for *swop*1 and *swop*2 are shown, but identical results were obtained for *swop*3. Numbers on the right show molecular weights (in thousands).

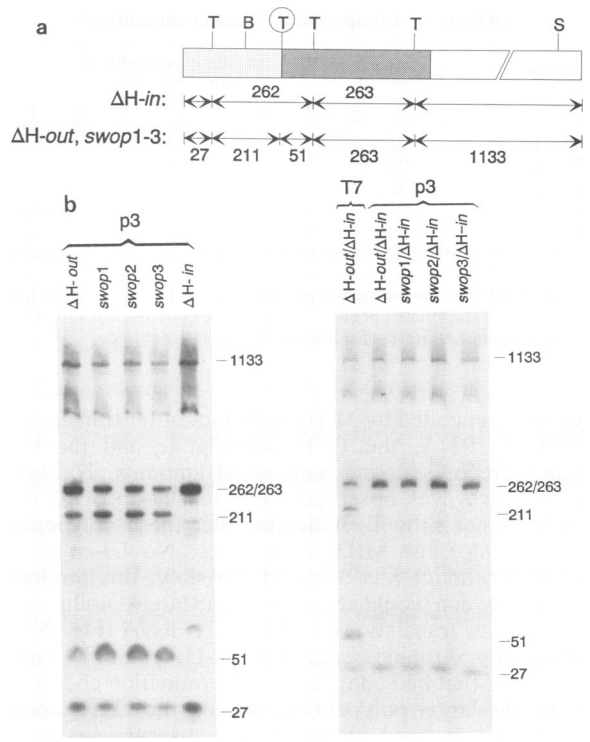

FIG. 5. *Taq*I analysis of RT-PCR DNA derived from p3 ΔH-*in* and ΔH-*out* DI RNA. The p3 RNAs described in the legend to Fig. 4 were subjected to RT-PCR with oligonucleotides 1 and 3. (a) Schematic representation of the resulting 1.7-kb PCR DNA fragment. The *Taq*I sites are indicated (T), as are the expected lengths of the restriction fragments generated upon *Taq*I digestion. The diagnostic *Taq*I site located at the ORF1a/1b junction of ΔH-*out* and its homologs *swop*1 to -3 is encircled. *Bss*HII (B) and *Sac*I (S) sites are also shown. (b) *Taq*I digestion of 1.7-kb RT-PCR DNA derived from p3 RNA (p3) or synthetic RNA (T7). The p3 RNA templates for RT-PCR were isolated after an initial transfection with a single DI RNA species (left panel) or a mixture of out-of-frame and in-frame DI RNAs (right panel); out-of-frame DI RNAs were transfected in 10-fold molar excess. Restriction fragments were labeled with [^{32}P]dCTP and Klenow DNA polymerase and analyzed in nondenaturing 5% polyacrylamide gels (30). Numbers on the right show fragment sizes (in nucleotides).

RNA was transfected in 10-fold molar excess, translation of p3 RNA yielded only the 110K polypeptide (Fig. 3b).

In principle, the poor propagation of ΔH-*out* could be caused by mutations that had been acquired inadvertently during the cloning procedures. To rule this out, we placed the out-of-frame ORF1a/1b junction of ΔH-*out* into the genetic background of ΔH-*in*. This was done by exchanging the 0.6-kb *Xho*I-*Mlu*I fragment of pΔH-*in* for the corresponding fragment of pΔH-*out* (Fig. 4a). Thus, three new out-of-frame clones were isolated that were designated p*swop*1, -2, and -3. RNAs transcribed from p*swop*1 to -3 were cotransfected in 10-fold molar excess with RNA from the parental construct pΔH-*in* and compared in a competition assay. Again, in vitro translation of p3 RNA yielded only the 110K polypeptide (Fig. 4b).

Strikingly, when MHV-A59-infected cells were transfected solely with the out-of-frame ΔH-*out* and *swop*1 to -3 DI RNAs, in vitro translation of the resulting p3 RNAs also yielded a 110K polypeptide; only trace amounts of the expected 66K polypeptide were detected (Fig. 3b and 4b). To exclude the possibility that contamination with ΔH-*in* had occurred during the transfection-propagation experiment, we analyzed the p3 DI RNAs in more detail. cDNA derived from ΔH-*out* and *swop*1 to -3 contains a *Taq*I site at the ORF1a/1b junction, which can be used to distinguish these DI RNAs from ΔH-*in* RNA (Fig. 3a and 5a). P3 RNA was subjected to DI-specific RT-PCR with oligonucleotides 1 and 3 (Table 1; Fig. 5a). *Taq*I digestion of the 1.7-kb RT-PCR products yielded restriction fragments of 211 and 51 bp, indicating that the ΔH-*out*-specific *Taq*I site had been retained (Fig. 5b, left). These results suggested that during passage of ΔH-*out* and *swop*1 to -3, escape mutants had been selected for that had restored the full-length ORF by a compensating frameshift mutation. As explained in Fig. 6a, such a frameshift could only have occurred within a defined 64-nucleotide region. Therefore, sequence analysis of this region was performed with cloned RT-PCR DNA as the template. For the majority of DI RNAs, the reading frame

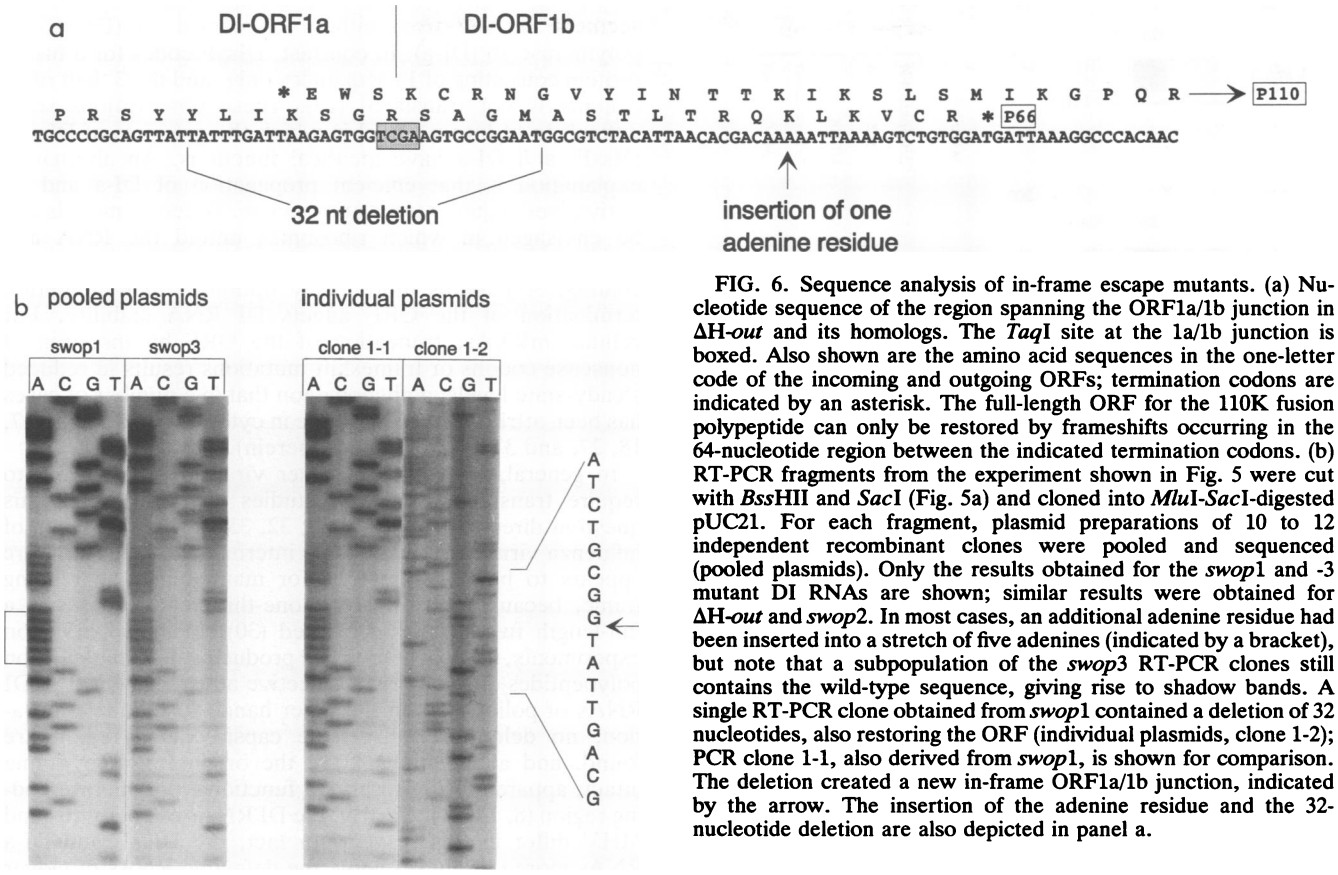

FIG. 6. Sequence analysis of in-frame escape mutants. (a) Nucleotide sequence of the region spanning the ORF1a/1b junction in ΔH-*out* and its homologs. The *Taq*I site at the 1a/1b junction is boxed. Also shown are the amino acid sequences in the one-letter code of the incoming and outgoing ORFs; termination codons are indicated by an asterisk. The full-length ORF for the 110K fusion polypeptide can only be restored by frameshifts occurring in the 64-nucleotide region between the indicated termination codons. (b) RT-PCR fragments from the experiment shown in Fig. 5 were cut with *Bss*HII and *Sac*I (Fig. 5a) and cloned into *Mlu*I-*Sac*I-digested pUC21. For each fragment, plasmid preparations of 10 to 12 independent recombinant clones were pooled and sequenced (pooled plasmids). Only the results obtained for the *swop*1 and -3 mutant DI RNAs are shown; similar results were obtained for ΔH-*out* and *swop*2. In most cases, an additional adenine residue had been inserted into a stretch of five adenines (indicated by a bracket), but note that a subpopulation of the *swop*3 RT-PCR clones still contains the wild-type sequence, giving rise to shadow bands. A single RT-PCR clone obtained from *swop*1 contained a deletion of 32 nucleotides, also restoring the ORF (individual plasmids, clone 1-2); PCR clone 1-1, also derived from *swop*1, is shown for comparison. The deletion created a new in-frame ORF1a/1b junction, indicated by the arrow. The insertion of the adenine residue and the 32-nucleotide deletion are also depicted in panel a.

had been restored by insertion of an extra adenine residue into a stretch of five. One PCR clone derived from *swop*1 RNA contained a 32-nucleotide deletion that also restored the ORF (Fig. 6).

These results raised the question whether escape mutants had emerged during the mixed transfection-propagation experiments as well. Figure 5b shows that when the out-of-frame ΔH-*out* and *swop*1 to -3 DI RNAs were cotransfected in a 10:1 ratio with ΔH-*in* RNA, PCR fragments derived from the resulting p3 DI RNAs lacked the *Taq*I site, which implies that ΔH-*in* had outcompeted the out-of-frame DI viruses. Apparently, the presence of the efficiently replicating ΔH-*in* prevented accumulation of ΔH-*out* and *swop*1 to -3 escape mutants.

Analysis of DI RNAs containing termination codons at two additional positions in the reading frame. Termination of the ORF immediately downstream of the ORF1a/1b junction clearly conferred a selective disadvantage to ΔH-*out*. We next asked whether termination at a position further downstream would also result in decreased fitness. For this purpose, we constructed two ΔH-*in* derivatives in which the ORF was truncated by creating frameshifts at the unique *Mlu*I and *Spe*I sites, thus allowing partial translation of ORF1b and N sequences (Fig. 7a). The resulting DI RNAs ΔH-*Mlu* and ΔH-*Spe*, containing ORFs for 81- and 92-kDa polypeptides, respectively, were compared with ΔH-*in* in a cotransfection-propagation assay (Fig. 2a); the out-of-frame DI RNAs were transfected in well over 10-fold molar excess. As shown in Fig. 7b, both ΔH-*Mlu* and ΔH-*Spe* were outcompeted by the parental DI virus, suggesting that translation of the 3′ end of the fusion ORF is required for efficient propagation.

DISCUSSION

The genome of the natural MHV DI virus DI-a contains a full-length fusion ORF encoding a 184K hybrid polypeptide (38). Here, we studied whether translation of this ORF is important for DI replication. For this purpose, we used pMIDI, a cDNA construct from which DI-a RNA can be transcribed in vitro (38), and a number of pMIDI derivatives. Comparison of pairs of nearly identical in-frame and out-of-frame DI RNAs showed that the ORF is indeed required for efficient propagation. Truncation of the ORF such that 1b and N sequences were not translated was not lethal but consistently led to reduced accumulation of DI RNA during transfection-propagation experiments. This was observed not only for MIDI-U (Fig. 2b) but also for ΔH-*out* and its homologs *swop*1 to -3 (data not shown). Moreover, when ΔH-*in* was directly compared to out-of-frame derivatives in cotransfection-propagation experiments, the in-frame DI ΔH-*in* prevailed within three successive passages, even when synthetic RNA of the out-of-frame DIs was transfected in large excess. The difference in fitness between in-frame and out-of-frame DIs was also illustrated by the fact that MIDI-C rapidly outcompeted the natural DI, DI-*en*, whereas DI-*en* could accumulate to large amounts in transfection-propagation experiments involving MIDI-U. Finally, during passage of DI viruses containing an out-of-frame genomic RNA, mutants emerged that had restored the reading frame. In MIDI-U, the termination codon was replaced by the wild-type sequence via homologous recombination between

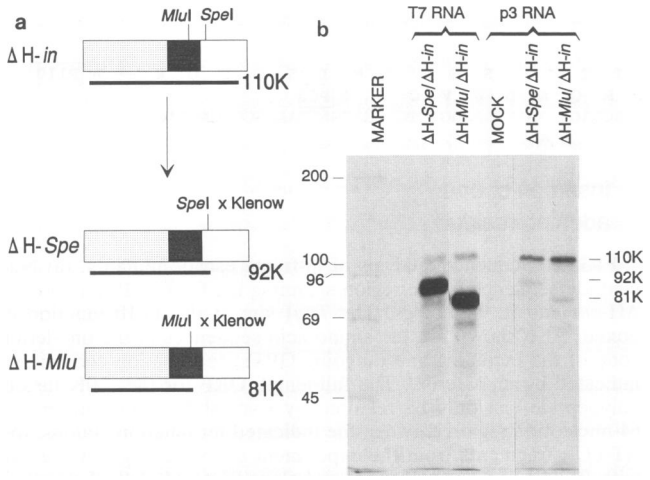

FIG. 7. ΔH-*in* derivatives containing frameshifts at the *Mlu*I and *Spe*I sites exhibit decreased fitness compared with the parental DI RNA. (a) Schematic representation of the construction of ΔH-*Spe* and ΔH-*Mlu*. pΔH-*in* DNA was digested with either *Spe*I or *Mlu*I. The 3′ recessed ends were filled in with Klenow DNA polymerase, after which the plasmid DNA was religated and cloned. ORFs are depicted as black bars. The molecular weights of the encoded fusion polypeptides are indicated. (b) pΔH-*Spe* and pΔH-*Mlu* DNA were mixed in large excess with the parental pΔH-*in* DNA and used for T7 transcription in vitro. The resulting synthetic RNA mixtures were translated in vitro, and the translation products were analyzed directly by SDS-PAGE (lanes marked T7 RNA). The RNA mixtures were then used for a cotransfection-propagation experiment as described in the legend to Fig. 2a. p3 RNA was isolated and translated in vitro. The DI-encoded products were immunoprecipitated with αP28 antiserum and analyzed (lanes p3 RNA). Numbers on the left show molecular weights (in thousands).

DI RNA and the standard virus genome, whereas for ΔH-*out* and *swop*1 to -3, the full-length ORF was restored by frameshift mutations. In most cases, a frameshift was achieved by insertion of a single adenine residue into a stretch of five adenines located immediately downstream of the artificial ORF1a/1b junction. It is unclear whether this insertion was made in vitro during transcription by T7 RNA polymerase, or in vivo. The fact that in-frame escape mutants were selected for strongly suggests that the decreased fitness of MIDI-U and ΔH-*out* compared with their in-frame counterparts MIDI-C and ΔH-*in* is due to truncation of the ORF rather than to differences in DI RNA structure. Intriguingly, the frameshift mutations in ΔH-*Mlu* and ΔH-*Spe* prevent translation of only the 3′-most 250 and 128 codons of the ΔH-*in* fusion ORF but still result in a decrease of fitness, suggesting that translation of the N sequences is essential for efficient propagation of DI-a derivatives.

Why does disruption of the fusion ORF impair DI replication? One interpretation is that the ORFs of DI-a and its derivatives encode functional proteins that augment DI propagation via a mechanism(s) yet to be defined. Indeed, the 184K polypeptide of DI-a was detected in infected cells by metabolic labeling (40). Fusion proteins encoded by two other natural MHV DIs, DIssF and DIssE, have also been found in infected cells, which likewise has prompted speculation on a possible role in DI replication (23, 24). Puzzlingly, however, the polypeptides of DIssE, DIssF, and DI-a differ significantly in structure. DI-a and DIssE code for fusion proteins composing the N terminus of the polymerase 1a protein, the C terminus of the N protein, and a middle segment derived from either polymerase 1a (DIssE) or polymerase 1b (DI-a). In contrast, DIssF codes for a fusion protein consisting of 1a sequences only, and the 3′ half of its genome is not translated (23). These observations seem difficult to fit into a model in which the products of DIssE, DIssF, and DI-a have identical functions. An alternative explanation is that efficient propagation of DI-a and its derivatives requires translation per se. Different models can be envisaged in which ribosomes unfold the RNA and thereby facilitate DI RNA amplification, packaging, or uncoating. A perhaps more likely option is that premature termination of the ORF affects DI RNA stability. For cellular mRNAs, truncation of the ORF by insertion of nonsense codons or frameshift mutations results in reduced steady-state levels, a phenomenon that in a number of cases has been attributed to a decrease in cytoplasmic half-life (17, 18, 27, and 37 and references therein).

In general, DI RNAs of other viruses do not seem to require translation, but few studies have addressed this question directly (7, 10, 29, 30, 32, 35). Most DI RNAs of influenza virus arise by a single internal deletion, and there appears to be no preference for maintaining the reading frame, because only in about one-third of the cases is a full-length fusion ORF generated (30). In mixed infection experiments, influenza virus DIs producing detectable fusion polypeptides did not have a selective advantage (1). The DI RNAs of poliovirus, on the other hand, do require translation; no deletions outside the capsid-coding region are found, and all deletions leave the original reading frame intact, apparently to preserve a functional polymerase-coding region (8, 13, 14). Clearly, the DI RNAs of poliovirus and MHV differ in this respect. In fact, the DIssE and DI-a RNAs more closely resemble the defective RNAs of clover yellow mosaic virus (41). The clover yellow mosaic virus defective RNAs are also of the 5′-3′ in-frame deletion type, containing full-length fusion ORFs that are crucial for propagation and/or accumulation in planta: synthetic defective RNAs in which the ORF was disrupted were nonviable (42).

In summary, we showed that the fitness of DI-a and its synthetic derivatives is decreased by frameshift and nonsense mutations in the fusion ORF. The precise role of this ORF remains obscure, however. Premature termination of translation may decrease DI RNA stability, but alternatively, the encoded protein may have some function in DI replication. Clearly, further studies are required to settle this issue.

ACKNOWLEDGMENTS

R. J. de Groot and R. G. van der Most contributed equally to this work.

We thank Susan Baker and Kathryn Holmes for kindly providing antisera against P28 and the N protein, Heleen Gerritsma for technical assistance, and Willem Luytjes for stimulating discussions and critical reading of the manuscript.

R.J.D.G. was supported by the Institute of Serology, Veterinary Faculty, Utrecht University. R.G.V.D.M. was supported by grant 331-020 from the Dutch Foundation for Chemical Research (SON).

REFERENCES

1. **Akkina, R. K., T. M. Chambers, and D. P. Nayak.** 1984. Expression of defective-interfering influenza virus-specific transcripts and polypeptides in infected cells. J. Virol. **51**:395–403.
2. **Ausubel, F. M.** 1989. Current protocols in molecular biology. Greene Publishing Associates and Wiley-Interscience, New York.
3. **Baker, S. C., and M. M. C. Lai.** 1990. An in vitro system for the leader-primed transcription of coronavirus mRNAs. EMBO J. **9**:4173–4179.

4. **Baker, S. C., C. K. Shieh, L. H. Soe, M. F. Chang, D. M. Vannier, and M. M. Lai.** 1989. Identification of a domain required for autoproteolytic cleavage of murine coronavirus gene A polyprotein. J. Virol. **63**:3693–3699.
5. **Denison, M., and S. Perlman.** 1987. Identification of putative polymerase gene product in cells infected with murine coronavirus A59. Virology **157**:565–568.
6. **Denison, M. R., and S. Perlman.** 1986. Translation and processing of mouse hepatitis virus virion RNA in a cell-free system. J. Virol. **60**:12–18.
7. **Dimmock, N. J.** 1991. The biological significance of defective interfering viruses. Rev. Med. Virol. **1**:165–176.
8. **Hagino-Yamagishi, K., and A. Nomoto.** 1989. In vitro construction of poliovirus defective interfering particles. J. Virol. **63**: 5386–5392.
9. **Hofmann, M. A., P. B. Sethna, and D. A. Brian.** 1990. Bovine coronavirus mRNA replication continues throughout persistent infection in cell culture. J. Virol. **64**:4108–4114.
10. **Holland, J. J.** 1991. Defective viral genomes, p. 151–165. *In* B. N. Fields, D. M. Knipe, et al. (ed.), Fundamental virology. Raven Press, New York.
11. **Huang, A. S., and D. Baltimore.** 1970. Defective viral particles and viral disease processes. Nature (London) **226**:325–327.
12. **Huang, A. S., and D. Baltimore.** 1977. Defective interfering animal viruses, p. 73–116. *In* H. Fraenkel-Conrat and R. R. Wagner (ed.), Comprehensive virology. Plenum Publishing Corp., New York.
13. **Kaplan, G., and V. R. Racaniello.** 1988. Construction and characterization of poliovirus subgenomic replicons. J. Virol. **62**:1687–1696.
14. **Kuge, S., I. Saito, and A. Nomoto.** 1986. Primary structure of poliovirus defective-interfering particle genomes and possible generation mechanisms of the particles. J. Mol. Biol. **192**:437–487.
15. **Lai, M. M. C., R. S. Baric, S. Makino, J. G. Keck, J. Egbert, J. L. Leibowitz, and S. A. Stohlman.** 1985. Recombination between nonsegmented RNA genomes of murine coronaviruses. J. Virol. **56**:449–456.
16. **Lee, H. J., C. K. Shieh, A. E. Gorbalenya, E. V. Koonin, N. LaMonica, J. Tuler, A. Bagdzhadzhyan, and M. M. C. Lai.** 1991. The complete sequence (22 kilobases) of murine coronavirus gene-1 encoding the putative proteases and RNA polymerase. Virology **180**:567–582.
17. **Lim, S.-K., C. D. Sigmund, K. W. Gross, and L. E. Maquat.** 1992. Nonsense codons in human β-globin mRNA result in the production of mRNA degradation products. Mol. Cell. Biol. **12**:1149–1161.
18. **Losson, R., and F. Lacroute.** 1979. Interference of nonsense mutations with eukaryotic messenger RNA stability. Proc. Natl. Acad. Sci. USA **76**:5134–5137.
19. **Makino, S., N. Fujioka, and K. Fujiwara.** 1985. Structure of the intracellular defective viral RNAs of defective interfering particles of mouse hepatitis virus. J. Virol. **54**:329–336.
20. **Makino, S., M. Joo, and J. K. Makino.** 1991. A system for study of coronavirus mRNA synthesis: a regulated, expressed subgenomic defective interfering RNA results from intergenic site insertion. J. Virol. **65**:6031–6041.
21. **Makino, S., J. G. Keck, S. A. Stohlman, and M. M. C. Lai.** 1986. High-frequency RNA recombination of murine coronaviruses. J. Virol. **57**:729–737.
22. **Makino, S., and M. M. C. Lai.** 1989. High-frequency leader sequence switching during coronavirus defective interfering RNA replication. J. Virol. **63**:5285–5292.
23. **Makino, S., C. Shieh, J. G. Keck, and M. M. C. Lai.** 1988. Defective-interfering particles of murine coronavirus: mechanism of synthesis of defective viral RNAs. Virology **163**:104–111.
24. **Makino, S., C. Shieh, L. H. Soe, S. C. Baker, and M. M. C. Lai.** 1988. Primary structure and translation of a defective interfering RNA of murine coronavirus. Virology **166**:1–11.
25. **Makino, S., F. Taguchi, and K. Fujiwara.** 1984. Defective interfering particles of mouse hepatitis virus. Virology **133**:9–17.
26. **Makino, S., K. Yokomori, and M. M. C. Lai.** 1990. Analysis of efficiently packaged defective interfering RNAs of murine coronavirus: localization of a possible RNA-packaging signal. J. Virol. **64**:6045–6053.
27. **Maquat, L. E., A. J. Kinniburgh, E. A. Rachmilewitz, and J. Ross.** 1981. Unstable beta-globin mRNA in mRNA-deficient β°-thalassemia. Cell **27**:543–553.
28. **Meinkoth, J., and G. Wahl.** 1984. Hybridization of nucleic acids immobilized on solid supports. Anal. Biochem. **138**:267–284.
29. **Monroe, S. S., and S. Schlesinger.** 1984. Common and distinct regions of defective-interfering RNAs of Sindbis virus. J. Virol. **49**:865–872.
30. **Nayak, D. P., T. M. Chambers, and R. M. Akkina.** 1989. Structure of defective-interfering RNAs of influenza virus and their role in interference, p. 269–317. *In* R. M. Krug (ed.), The influenza viruses. Plenum Press, New York.
31. **Pachuk, C. J., P. J. Bredenbeek, P. W. Zoltick, W. J. M. Spaan, and S. R. Weiss.** 1989. Molecular cloning of the gene encoding the putative polymerase of mouse hepatitis coronavirus, strain A59. Virology **171**:141–148.
32. **Roux, L., A. E. Simon, and J. J. Holland.** 1991. Effects of defective interfering viruses on virus replication and pathogenesis in vitro and in vivo. Adv. Virus Res. **40**:181–211.
33. **Sambrook, J., E. F. Fritsch, and T. Maniatis.** 1989. Molecular cloning: a laboratory manual, 2nd ed. Cold Spring Harbor Laboratory, Cold Spring Harbor, N.Y.
34. **Sawicki, S. G., and D. L. Sawicki.** 1990. Coronavirus transcription: subgenomic mouse hepatitis virus replicative intermediates function in RNA synthesis. J. Virol. **64**:1050–1056.
35. **Snijder, E. J., J. A. den Boon, M. C. Horzinek, and W. J. M. Spaan.** 1991. Characterization of defective interfering RNAs of Berne virus. J. Gen. Virol. **72**:1635–1643.
36. **Spaan, W. J. M., P. J. M. Rottier, M. C. Horzinek, and B. A. M. van der Zeijst.** 1981. Isolation and identification of virus-specific mRNAs in cells infected with mouse hepatitis virus (MHV-A59). Virology **108**:424–434.
37. **Vancanneyt, G., S. Rosahl, and L. Willmitzer.** 1990. Translatability of a plant-mRNA strongly influences its accumulation in transgenic plants. Nucleic Acids Res. **18**:2917–2921.
38. **van der Most, R. G., P. J. Bredenbeek, and W. J. M. Spaan.** 1991. A domain at the 3′ end of the polymerase gene is essential for encapsidation of coronavirus defective interfering RNAs. J. Virol. **65**:3219–3226.
39. **van der Most, R. G., L. Heijnen, W. J. M. Spaan, and R. J. de Groot.** 1992. Homologous RNA recombination allows efficient introduction of site-specific mutations into the genome of coronavirus MHV-A59 via synthetic co-replicating RNAs. Nucleic Acids Res. **20**:3375–3381.
40. **van der Most, R. G.** Unpublished data.
41. **White, K. A., J. B. Bancroft, and G. A. Mackie.** 1991. Defective RNAs of clover yellow mosaic virus encode nonstructural/coat protein fusion products. Virology **183**:479–486.
42. **White, K. A., J. B. Bancroft, and G. A. Mackie.** 1992. Coding capacity determines in vivo accumulation of a defective RNA of clover yellow mosaic virus. J. Virol. **66**:3069–3076.